Formation of racemic compound crystals by mixing of two enantiomeric crystals in the solid state. Liquid transport of molecules from crystal to crystal

Fumio Toda,*[a] Koichi Tanaka,[a] Hisakazu Miyamoto,[a] Hideko Koshima,[b] Ikuko Miyahara[c] and Ken Hirotsu[c]

[a] *Department of Applied Chemistry, Faculty of Engineering, Ehime University, Matsuyama, Ehime 790, Japan*
[b] *Department of Materials Chemistry, Faculty of Science and Technology, Ryukoku University, Otsu, Shiga, Japan*
[c] *Department of Chemistry, Faculty of Science, Osaka City University, Sugimotocho, Osaka, Japan*

Mixing of powdered (−)- and (+)-enantiomer crystals in the solid state gives crystals of the racemic compound. This racemic crystal formation was followed by IR spectral measurement of a 1:1 mixture of (−)- and (+)-enantiomer crystals as a Nujol mull. As the formation of racemic crystals proceeds, the OH absorptions of the enantiomer disappear gradually and new OH absorptions due to the racemic compound appear. The formation of racemic crystals from enantiomer crystals has been studied for various kinds of chiral compounds: 2,2′-dihydroxy-1,1′-binaphthyl (1) and its derivatives, 10,10′-dihydroxy-9,9′-biphenanthryl (4), 2,2′-dihydroxy-4,4′,6,6′-tetramethylbiphenyl (5) and its derivatives, 4,4′-dihydroxy-2,2′,3,3′,6,6′-hexamethylbiphenyl (8), 1,6-di(*o*-chlorophenyl)-1,6-diphenylhexa-2,4-diyne-1,6-diol (11) and its derivatives, *trans*-4,5-bis[hydroxy(diphenyl)methyl]-2,2-dimethyl-1,3-dioxacyclopentane (17) and its derivatives, tartaric acid (20) dimethyl tartrate (21), malic acid (22), mandelic acid (23), and norephedrine (24). These molecular movements and blending occur rapidly in the presence of liquids such as liquid paraffin (Nujol), seed oils such as olive, coconut, rapeseed and soybean oil, artificial oil such as silicone oil and water, although the same movement also occurs in the absence of the liquid. For example, keeping a mixture of powdered (−)-1 (1a) and (+)-1 (1b) at room temperature for 48 h gives racemic crystals (1c). However, molecular aggregation sometimes occurs in solution but not in the solid state. For example, recrystallization of (−)-16 (16a) and (+)-16 (16b) from solvent gives racemic crystals of 16c, although mixing of these two components as powders in the presence of liquid does not give 16c. In order to determine the mechanism of the molecular movement in the solid state, X-ray crystal structures of optically active and racemic compounds and also the molecular movements from optically active crystal to racemic crystal have been studied.

Introduction

Because of the strong influence of the famous Aristotelian philosophy *No coopora nisi fluida* which means 'no reaction occurs in the absence of solvent', most organic reactions have been studied in solution. We have found, however, that many organic reactions can be carried out in the absence of solvent and that indeed many solid state reactions proceed more selectively and efficiently than do solution reactions.[1] Such solid state reactions show that molecules move easily from reagent crystal to reactant crystal. After this molecular movement, reaction occurs on the surface of the reactant crystal. This process has been studied by AFM (atomic force microscopy) experiments.[2] The molecular movement in the solid state[3] has also been observed spectroscopically. For example, host–guest inclusion complexation in the solid state can be followed by IR[4] or UV[5] spectroscopy. Host–guest inclusion complexation in the solid state proceeds stereo- and enantio-selectively. When powdered optically active host crystals are mixed with powdered racemic guest crystals, enantioselective molecular movement occurs and optical resolution of the racemic guest compound can be accomplished in the solid state.[6] By a combination of the enantioselective molecular movement in the solid state and fractional distillation, optical resolution can be achieved by distillation in the presence of an optically active host.[7] By mixing an optically active host and racemic guest in the solid state, one enantiomer of the guest forms an inclusion complex with the host by molecular movement and then the uncomplexed enantiomer distils at a relatively low temperature without degradation of the inclusion complex. By further heating at a relatively high temperature, the inclusion complex decomposes and the complexed enantiomer distils out. By this method, very efficient resolution of various kinds of guest compounds has been accomplished.[8] By a similar procedure, stereoisomers with the same or very similar boiling points can be separated by distillation in the presence of a host compound. Much more interesting molecular movement in the solid state occurs between a chiral host and prochiral guest. Mixing of powdered optically active host and prochiral guest gives the host–guest inclusion complex in which the latter molecules are arranged in a chiral form and which upon photoirradiation in the solid state gives an optically active photoreaction product.[9] Formation of charge-transfer (CT) complex crystals by mixing powdered acceptor and donor crystals in the solid state has also been known for a long time. Quinhydrone is easily formed by mixing hydroquinone and benzoquinone crystals in the solid state.[10] Formation of various CT complex crystals by the mixing method has been reported,[11] and the CT complex crystals produced by the mixing method showed comparable electrical conductivity to that of the complex prepared by crystallization of the components from a solvent.[12] Formation of co-crystals of nitrobenzoic acid derivatives with anthracene by mixing both components in the solid state has also been reported.[13]

In order to understand the molecular movement from crystal to crystal more precisely, we studied formation of racemic host compound crystals by mixing two enantiomer crystals in the solid state using IR spectroscopic and X-ray crystal structural studies. We mostly studied the formation of racemic host crystals from (−)- and (+)-host crystals. During these studies on molecular movement, we found that the formation of racemic crystals from enantiomer crystals is accelerated by liquids such as liquid paraffin, seed oil, silicone oil, and water, although the same phenomenon also occurs slowly in the absence of the liquid.

Experimental

Materials

Optically active 2,2′-dihydroxy-1,1′-binaphthyl (**1a**, **1b**) and its

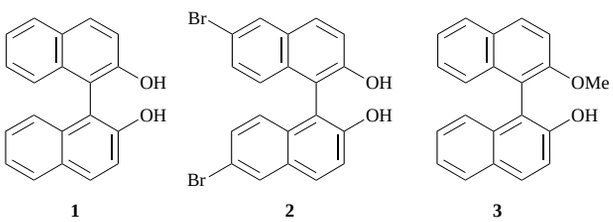

1 **2** **3**

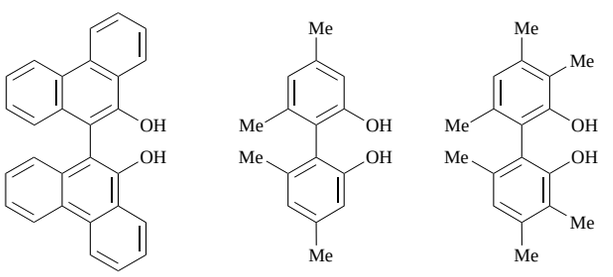

4 **5** **6**

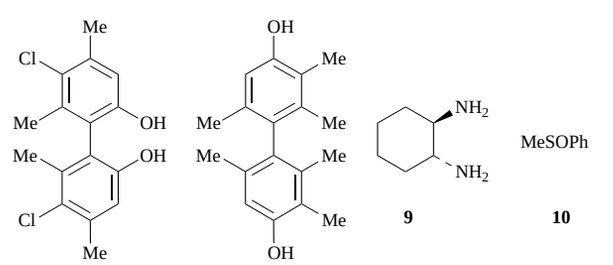

7 **8** **9** **10**

a (–)-form **b** (+)-form **c** (±)-form

6,6′-dibromo derivative (**2a**, **2b**) were prepared by optical resolution of their racemates **1c** and **2c**, respectively,[14] through inclusion complexation with *N*-benzylcinchonidinium chloride.[15] The monomethyl ether of **1a** and **1b** (**3a**, **3b**)[16] and of **1c** (**3c**)[17] were prepared according to the reported method. Optically active 10,10′-dihydroxy-9,9′-biphenanthryl (**4a**, **4b**) were prepared by resolution of its racemate (**4c**)[14] through complexation with *N*-butylcinchonidinium bromide.[15]

Optically active 2,2′-dihydroxy-4,4′,6,6′-tetramethylbiphenyl (**5a**, **5b**) and 4,4′-dihydroxy-2,2′,3,3′,6,6′-hexamethylbiphenyl (**8a**, **8b**) were prepared by optical resolution of their racemates by complexation with *N*-benzylcinchonidinium chloride and (−)-*trans*-2,3-bis[hydroxy(diphenyl)methyl]-1,4-dioxaspiro-[4.4]nonane (**18a**),[18] respectively, according to the reported method.[19] However, these methods were not applicable to the resolution of **6c** and **7c**. Optically active 3,3′,4,4′,6,6′-hexamethyl- (**6a**, **6b**) and 5,5′-dichloro-4,4′,6,6′-tetramethyl-2,2′-dihydroxybiphenyl (**7a**, **7b**) were obtained by complexation of their racemates with (−)-*trans*-1,2-diaminocyclohexane (**9a**).

When a solution of **9a** (0.63 g, 5.52 mmol) and **6c**[20] (2 g, 7.4 mmol) in toluene (0.3 ml) was kept at room temperature for 2 h, a 1:1 inclusion complex of **9a** and **6b** was obtained (1.18 g). Recrystallization of the crude crystal (1.18 g) from toluene gave pure crystals (0.8 g, mp 117–125 °C). These were dissolved in AcOEt (20 ml)–dil. HCl (20 ml), and the AcOEt layer was washed with water and dried over Na_2SO_4. Evaporation of the solvent from the dried AcOEt solution gave **6b** of 100% enantiomeric excess (ee) as colorless needles {0.39 g, 39% yield, mp 127 °C, $[\alpha]_D$ +23.7 (*c* 1.0, MeOH)}. The filtrate left after separation of the crude 1:1 complex of **9a** and **6b** was dissolved in AcOEt (20 ml)–dil. HCl (20 ml), and the AcOEt layer was washed with water and dried over Na_2SO_4. Evaporation of the filtrate from the dried AcOEt solution gave **6a** of 90% ee (0.88 g, 88% yield) which upon recrystallization from toluene gave **6a** of 100% ee (0.25 g, 25% yield). By a similar resolution, **7a** and **7b** of 100% ee were obtained. When a solution of **9a** (1.14 g, 9.98 mmol) and **7c**[19] (2 g, 6.68 mmol) in toluene (0.4 ml) was kept at room temperature for 5 h, a 2:1 crude complex of **9a** and **7b** was obtained, which upon two recrystallizations from toluene gave the pure complex (1.52 g, mp 116–117 °C). This pure complex (1.52 g) was dissolved in AcOEt (20 ml)–dil. HCl (20 ml), and the AcOEt layer was washed with water and dried over Na_2SO_4. Evaporation of the filtrate from the AcOEt solution gave **7b** of 100% ee as colorless needles {0.58 g, 58% yield, mp 235 °C, $[\alpha]_D$ +67.2 (*c* 1.0, MeOH)}. From the toluene solution left after separation of the crude 2:1 complex of **9a** and **7b**, **7a** of 100% ee (0.25 g, 25% yield) was obtained by the same procedure as that applied to the isolation of **6b**. Very interestingly, however, **9a** formed a 1:1 complex with racemic guest **7c**, although **9a** formed a 2:1 complex with optically active guest **7b** as described above. For example, when a solution of **9a** (0.76 g, 6.66 mmol) and **7c** (2g, 6.68 mmol) in toluene (0.3 ml) was kept at room temperature for 2 h, a 1:1 complex of **9a** and **7c** was formed as colorless needles (2.43 g, 88% yield), from which **7c** was isolated (1.6 g, 80% yield). The optical purity of **6** and **7** was determined by HPLC on the chiral stationary phase Chiralpak AS.[21]

Acetylenic alcohol host compounds (**11**, **12**, **14**–**16**) were pre-

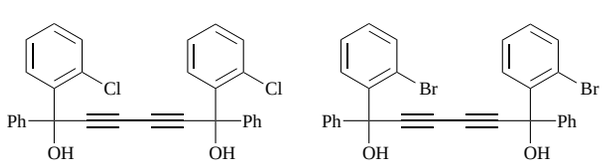

11 **12**

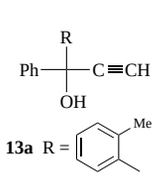

b R = H
c R = Bu^t

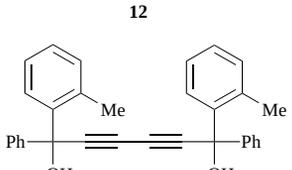

14

15

16

pared by the following method. Optically active 1,6-di(*o*-chlorophenyl)-1,6-diphenylhexa-2,4-diyne-1,6-diol (**11a**, **11b**), its bromoanalog (**12a**, **12b**), and 1,6-diphenyl-1,6-di(*tert*-butyl)-hexa-2,4-diyne-1,6-diol (**16a**, **16b**) were prepared according to the reported method.[22] Optically active 1,6-bis(*o*-tolyl)-1,6-diphenylhexa-2,4-diyne-1,6-diol (**14a**, **14b**) {mp 109–112 °C, $[\alpha]_D$ 19 (*c* 0.9, MeOH)} and 1,6-diphenylhexa-2,4-diyne-1,6-diol (**15a**, **15b**) {mp 118–120 °C, $[\alpha]_D$ 0.4 (*c* 0.6, MeOH)} were

prepared by $CuCl_2$-catalyzed coupling reaction in pyridine of the optically active 1-(*o*-tolyl)-1-phenylprop-2-yn-1-ol (**13a**)[23] and 1-phenylhexa-2,4-diyne-1,6-diol (**13b**),[24] respectively.

Optically active *trans*-4,5-bis[hydroxy(diphenyl)methyl]-2,2-dimethyl-1,3-dioxacyclopentane (**17a**, **17b**)[18,25] and *trans*-2,3-bis[hydroxy(diphenyl)methyl]-1,4-dioxaspiro[5.4]decane (**19a**, **19b**)[18,25] were prepared according to the reported methods.

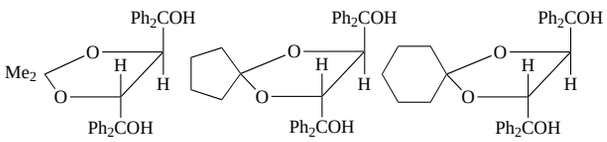

17 **18** **19**

a (–)-form **b** (+)-form **c** (±)-form

Commercially available samples of optically active tartaric acid (**20**), dimethyl tartrate (**21**), malic acid (**22**), mandelic acid (**22**), and norephedrine (**24**) were used for the experiments.

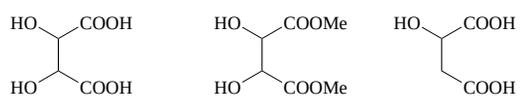

20 **21** **22**

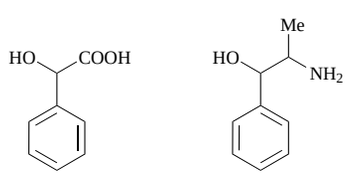

23 **24**

Cocrystallizations

Powdered (−)- and (+)-crystals (5 mg each) were mixed with liquid paraffin (20 mg) to give the Nujol mull as a paste, the IR spectrum of which was recorded. Racemic crystals for X-ray analysis were prepared by recrystallization of the same amount of (−)- and (+)-enantiomeric crystals from the appropriate solvent, toluene or diethyl ether. For example, recrystallization of **16a** (100 mg) and **16b** (100 mg) from toluene (5 ml) gave **16c** as colorless prisms (140 mg, 70% yield, mp 141 °C).

IR spectra

All IR spectra were recorded on a Jasco FT-IR Spectrophotometer FT-IR 300 for Nujol mulls using NaCl windows unless otherwise stated. FT-IR spectra were recorded on a Shimazu FT-IR Spectrophotometer FT-IR 4200 in the absence of liquid paraffin.

X-Ray analyses

The single crystals suitable for X-ray analysis were obtained by recrystallization from EtOH for **1a**, from MeCN for **1c**, from toluene for **5b**, **5c**, **7b**, **7c**, 1:1 complex of **8b** with **10b**, **11c**, 1:1 cocrystal of **11b** and **12a**, **16b**, **16c**, **17a**, **19a**, and **19c**, from ether for **18a** and **18c**, and from EtCN for **17c**. All the data were collected on a Rigaku AFC7R four circle diffractometer with graphic monochromated Cu-Kα or Mo-Kα radiation and a rotating anode generator (50 KV, 200 mA). All these data are summarized in Table 1. The structures were solved using direct methods.[26] The non-hydrogen atoms were refined anisotropically and all the hydrogen atoms were included in the structure factor calculations, except for **11b**. No absorption correction was applied except that mentioned in the crystal data. All calculations were performed using the teXsan crystallographic software package.[27] Although X-ray data for **1a**,[28] and **17a** and **17c**[29] have been reported, we used our own data, because of their improved quality.

Results and discussion

Formation of 1c, 2c and 4c in the solid state

When IR spectra of a 1:1 mixture of **1a** and **1b** were measured as a Nujol mull every 5 min for 1 h, the OH absorptions of **1a** and **1b** at 3510 and 3435 cm^{-1} decreased gradually and finally disappeared after 1 h, and new OH absorptions of **1c** appeared at 3485 and 3405 cm^{-1} [Fig. 1(*a*)]. The latter two OH absorptions are identical to those of **1c** prepared by crystallization of **1a** and **1b** from a solvent. This result shows that optically active molecules of **1a** and **1b** move between their crystals and form

Table 1 Summary of crystal data

Compound	Space group	*a*/Å	*b*/Å	*c*/Å	*β*/° (or *α*, *β*, *γ*)	*Z*	D_c/g cm^{-3}	*R*
1a	$P3_2$	10.7953(9)	—	10.865(2)	—	3	1.301	0.038
1c	*Iba*2	21.592(3)	15.687(2)	8.617(1)	—	8	1.303	0.040
5b[a]	$P2_12_12_1$	8.905(1)	20.546(2)	7.463(1)	—	4	1.179	0.042
5c	$P2_1/c$	11.181(3)	7.652(3)	16.590(2)	106.43(1)	4	1.182	0.047
7b	$P2_12_12_1$	8.381(2)	8.522(3)	41.651(3)	—	8	1.390	0.058
7c	$P2_1/c$	8.561(3)	8.310(3)	21.093(5)	94.66(2)	4	1.382	0.064
8b·10b	$P2_1$	9.058(5)	11.050(3)	11.520(2)	97.23(3)	2	1.192	0.034
11a	$P2_12_12_1$	16.78(4)	41.5(2)	8.030(8)	—	8	1.147	0.171
11c	$C2/c$	21.209(2)	11.5299(9)	9.627(1)	93.910(9)	4	1.367	0.033
11b·12a	$C2$	21.189(3)	11.642(3)	9.619(2)	93.94(2)	4	1.481	0.025
16b	$P2_12_12_1$	14.048(3)	25.726(2)	6.069(2)	—	4	1.134	0.046
16c	$P\bar{1}$	12.209(2)	21.174(3)	9.282(1)	102.30(1) 97.35(1) 102.30(1)	4	1.105	0.071
17a	$P\bar{1}$	11.870(1)	12.847(1)	9.367(1)	97.36(1) 102.50(1) 109.084(9)	2	1.204	0.032
17c	$P\bar{1}$	11.324(3)	12.081(3)	9.679(2)	93.38(2) 105.07(2) 103.09(2)	2	1.254	0.048
18a	$C2$	15.700(2)	9.325(1)	18.455(1)	105.372(7)	4	1.256	0.035
18c	$P2_1/n$	14.042(2)	13.100(3)	14.400(2)	95.99(1)	4	1.242	0.058
19a	$P2_12_12_1$	10.212(4)	29.284(3)	9.314(2)	—	4	1.208	0.036
19c	$P\bar{1}$	12.3229(9)	13.1134(6)	9.1404(6)	93.099(5) 101.634(7) 107.339(5)	2	1.228	0.059

[a] Absolute configuration not determined

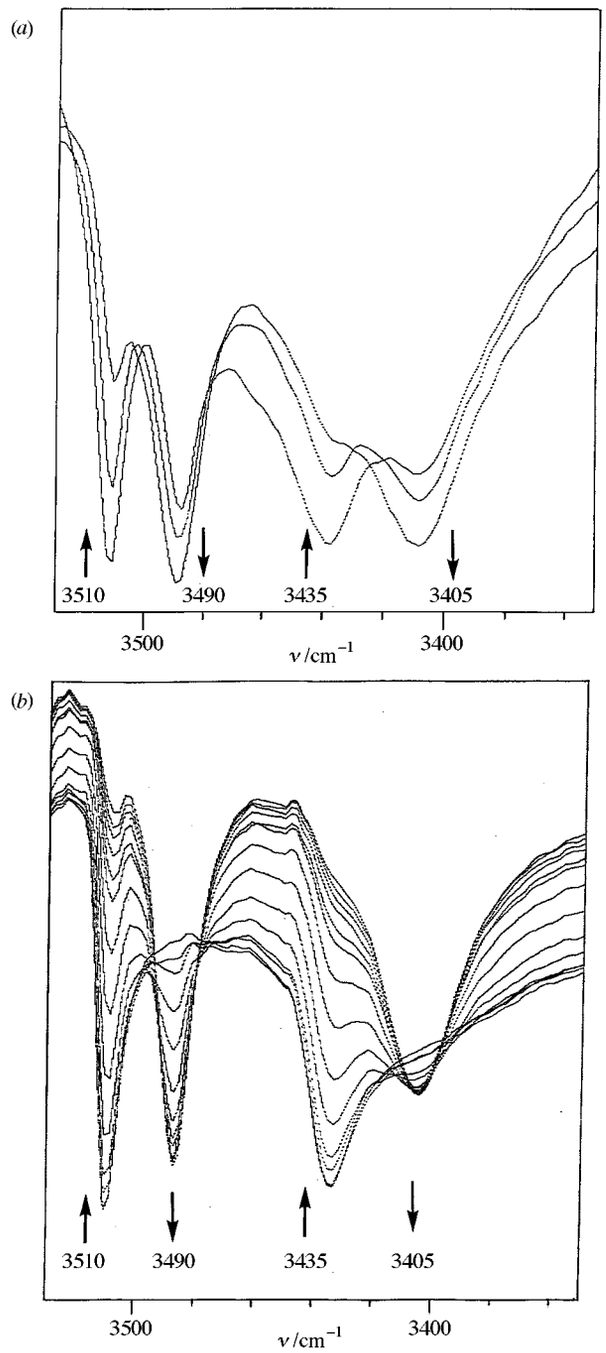

Fig. 1 IR spectra of a 1:1 mixture of **1a** and **1b**: in the absence (*a*) and presence (*b*) of liquid paraffin. Measured every 24 h for 48 h (*a*) and every 5 min for 1 h (*b*)

crystals of the racemic compound **1c** in the solid state. This molecular movement is surprisingly fast. This phenomenon is not special for **1** but rather common. When IR spectra of a 1:1 mixture of **2a** and **2b** were measured for 20 min, their OH absorptions at 3470 and 3430 cm^{-1} disappeared completely and new OH absorptions of **2c** appeared at 3455 cm^{-1}. Such molecular movement was also observed for **4**. During IR measurement of a 1:1 mixture of **4a** and **4b** for 1 h, their OH absorptions at 3520, 3500 and 3480 cm^{-1} disappeared completely and new absorptions for **4c** appeared at 3520, 3500 and 3485 cm^{-1}. The absorptions of **4c** were identical to those of the racemic compound prepared by crystallization of **4a** and **4b** from a solvent.

Since **3c** was not formed by mixing **3a** and **3b** in the solid state, the two hydroxy groups of **1**, **2** and **4** seem to be essential for the molecular movement. Furthermore, when IR spectra of a 1:1 mixture of **1a** and **1b** were measured in the absence of

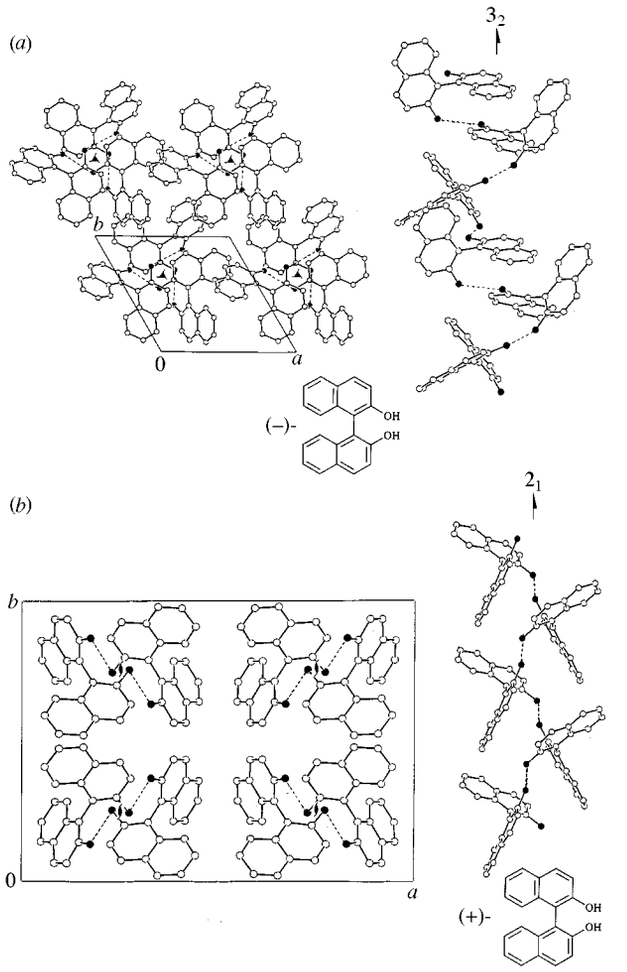

Fig. 2 (*a*) View of the crystal structure of **1a** along the *c*-axis and side view of the 3_2 helical structure formed by the hydrogen bonding between hydroxy groups of neighboring molecules. (*b*) View of the crystal structure of **1c** along the *c*-axis and the 2_1 helical structure consisting of **1b** molecules. Hydrogen bonds are shown by dotted lines and oxygen atoms by filled circles.

liquid paraffin by a diffraction method, it took 48 h to complete the formation of **1c** [Fig. 1(*b*)], although one hour is enough to complete the molecular movement for a Nujol mull. This strongly suggests that the molecular movement in the solid state occurs even in the absence of liquid such as liquid paraffin (Nujol), but is accelerated very much by a liquid.

In order to study the mechanism of the formation of **1c** crystals by molecular assembly between **1a** and **1b**, X-ray crystal structures of **1a** and **1c** were analyzed.[28] In **1a** crystals, the molecules are stacked around a 3_2 screw axis to form a left-handed helical structure through a hydrogen bond O–H · · · O of length 2.96 Å (Fig. 2). The dihedral angles between the two naphthalene rings are 101.7°. In **1c** crystals, **1a** and **1b** molecules with a dihedral angle of 90.6° from a typical hydrogen bonded helical structure along the 2_1 screw axis with O–H · · · O = 2.84 Å (Fig. 2). The crystal structure is characterized by the alternate packing of the helical structure consisting of **1a** molecules and that of **1b** molecules.

The inside of the 3_2 and 2_1 helical structures is hydrophilic and the outside is hydrophobic with van der Waals interactions only between the helical structures. Each diol molecule in the helical structure is hydrogen bonded to its neighboring molecules by one donor and one acceptor bond, resulting in one of the hydroxy hydrogen atoms being free from hydrogen bonding. From the crystal structural point of view, the formation of **1c** crystals from **1a** and **1b** crystals looks just like a mutual penetration of 3_1 and 3_2 helical structures through the interface between enantiomeric crystals, followed by the conversion of

three-fold screw structures into two-fold screw structures. Since the hydrogen bond is shorter in **1c** than in **1a**, the dihedral angle in **1c** is closer to rectangular than that in **1c** and the density of **1c** is slightly larger than that of **1a**. Hence the molecular packing in **1c** would be more favorable than that in **1a**. The two OH absorptions of **1a** at 3510 and 3435 cm^{-1} can be assigned to the stretching of the two OH groups which act as hydrogen acceptor and donor, respectively (Fig. 2). Similarly, the two OH absorptions of **1c** at 3470 and 3430 cm^{-1} are assignable to the two OH groups which are a hydrogen acceptor and a hydrogen donor, respectively (Fig. 2).

The difference in the heat of melting of **1c** (ΔH 32 kJ mol^{-1}) and **1a**, **1b** (ΔH 29 kJ mol^{-1}) recorded by DSC measurements also indicates that **1c** crystals are more stable than **1a** and **1b** crystals. The more stable structure of **1c** would be a driving force to cause molecular movement between **1a** and **1b** and the formation of **1c** in the solid state. Nevertheless, it is very interesting that the two chiral crystals in which **1a** and **1b** molecules are arranged so as to form a three-fold screw axis (clockwise and anti-clockwise, respectively) give racemic crystals **1c** in which two kinds of two-fold screw axes with alternate clockwise and anti-clockwise arrangements are produced just by mixing **1a** and **1b** crystals for a short time in the solid state.

Formation of 5c, 6c, 7c and 8c in the solid state

By successive IR spectral measurements of a 1:1 mixture of **5a** and **5b** in Nujol mulls every 5 min for 30 min, the original OH absorptions at 3480 and 3450 cm^{-1} turned into those of **5c** at 3480 and 3420 cm^{-1}. By similar measurements of a 1:1 mixture of **6a** and **6b** (3530, 3510 and 3460 cm^{-1}) for 30 min and of **7a** and **7b** (3495 and 3450 cm^{-1}) for 3 h, the OH absorptions indicated turned into those of **6c** at 3520, 3468 and 3420 cm^{-1} and those of **7c** at 3490 and 3430 cm^{-1}, respectively. The formation of **6c** is extremely fast. However, the formation of **8c** from **8a** and **8b** is relatively slow. When successive IR spectra of a 1:1 mixture of **8a** and **8b** were measured, the original OH absorption at 3270 cm^{-1} disappeared after 5 h and the new absorption of **8c** at 3185 cm^{-1} appeared.

X-Ray structures of **5b** and **5c** crystals are shown in Fig. 3. In **5b** crystals, a 2_1 helical structure similar to that consisting of **1b** molecules in **1c** crystals is created along the *c*-axis by the O–H · · · O hydrogen bonds (2.910 Å) between the neighboring **5b** molecules. The dihedral angle between the two phenyl rings of **5b** is 81.5°. The crystal structure of **5c** consists of an alternating arrangement of the 2_1 helical structures of opposite chirality. The helical structure consisting of **5b** in **5c** crystals is identical to that in the **5b** crystals. The dihedral angle between the two phenyl rings is 86.4° and the hydrogen bond distance is 2.878 Å.

In **5b** and **5c** crystals, the hydrophilic parts (two OH groups) of the molecules are located in the center of the helical columns and encircled by the large hydrophobic moieties, resulting in no participation of one of the two hydroxy hydrogens of the molecule in hydrogen bonding. This hydrogen is sandwiched between two benzene rings of the molecule and the neighboring one in the column. Only van der Waals interactions are observed between the helical structures. The **5c** crystal is modelled by replacing alternately the 2_1 helical structures in **5b** crystals by the 2_1 helical structures in **5a** crystals. The hydrogen bond is shorter in **5c** than in **5b**, the dihedral angle in **5c** is closer to a right angle than that in **5b**, and the density of **5c** is slightly larger than that of **5b**, suggesting that the molecular packing of **5c** will be more favorable than that of **5b**.

X-Ray crystal structures of **7b** and **7c** are shown in Fig. 4. The crystal structure of **7b** is complicated compared with that of **5b**, because the asymmetric unit contains two independent molecules. However, the independent **7b** molecules form similar 2_1 helical structures along the *a*- and *b*-axes to those found in **5b**, resulting in assembly of the mutually rectangular helical structures in the crystal. The dihedral angles between the two phenyl rings are 75.6 and 70.7°, and the hydrogen bond lengths

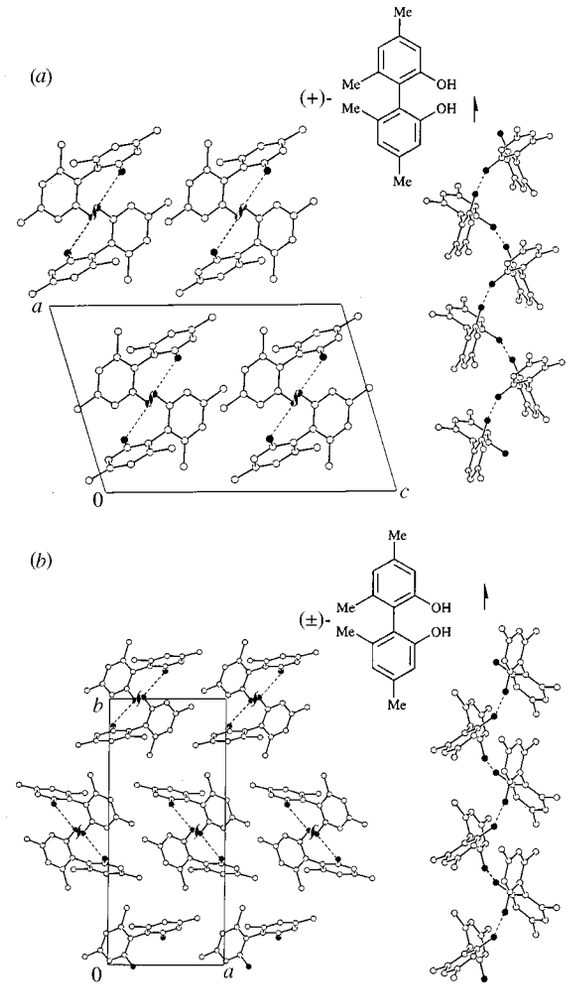

Fig. 3 (*a*) View of the crystal structure of **5b** along the *c*-axis and side view of the 2_1 helical structure formed by hydrogen bonding between hydroxy groups of neighboring molecules. Absolute configuration is not determined. (*b*) View of the crystal structure of **5c** along the *b*-axis and side view of the 2_1 helical structure in **5c** crystals. Hydrogen bonds are shown by dotted lines and oxygen atoms by filled circles.

are 2.880 and 2.909 Å. The crystal structure of **7c** is composed of alternate arrangements of the 2_1 helical structure with opposite chirality. The helical structure composed of **7b** in the **7c** crystals is the same as that in **7b** crystals. The dihedral angle between the two phenyl rings is 76.4° and the hydrogen bond length is 2.838 Å.

In **7b** and **7c** crystals, there are no special interactions between the helical structures except van der Waals interactions and one of the two hydroxy hydrogens of the molecule is free from hydrogen bonding as is observed in the crystal structures of **5b** and **5c**. The stacking of the helical structures along the *a*-axis of the **7c** crystals mimics those along the *a*- or *b*-axis of **7b**. As far as the hydrogen bond distances and the dihedral angles are concerned, the molecular packing of **7c** will be favorable compared with that of **7b**. The slow transformation from enantiomeric crystals of **7a** and **7b** to **7c** crystals might be at least in part due to the rectangular arrangements of the helical structure in the chiral crystal and the slightly larger density of **7b** than that of **7c**.

Since neither **8b** (nor **8a**) nor **8c** formed suitable crystals for a single X-ray crystal analysis, the 1:1 inclusion crystal of **8b** and optically pure (+)-methyl phenyl sulfoxide (**10b**)[19] was subjected to X-ray analysis. The packing of the 1:1 complex is shown in Fig. 5, from which the absolute configuration of **8b** was elucidated to be (*S*), because the configuration of **10b** is known as (*R*).[19] The packing of **8b** itself is also shown in Fig. 5, by excluding **10b** molecules for clarity. The molecules of **8b** are linked by hydrogen bonds to give a linear arrangement of **8b**

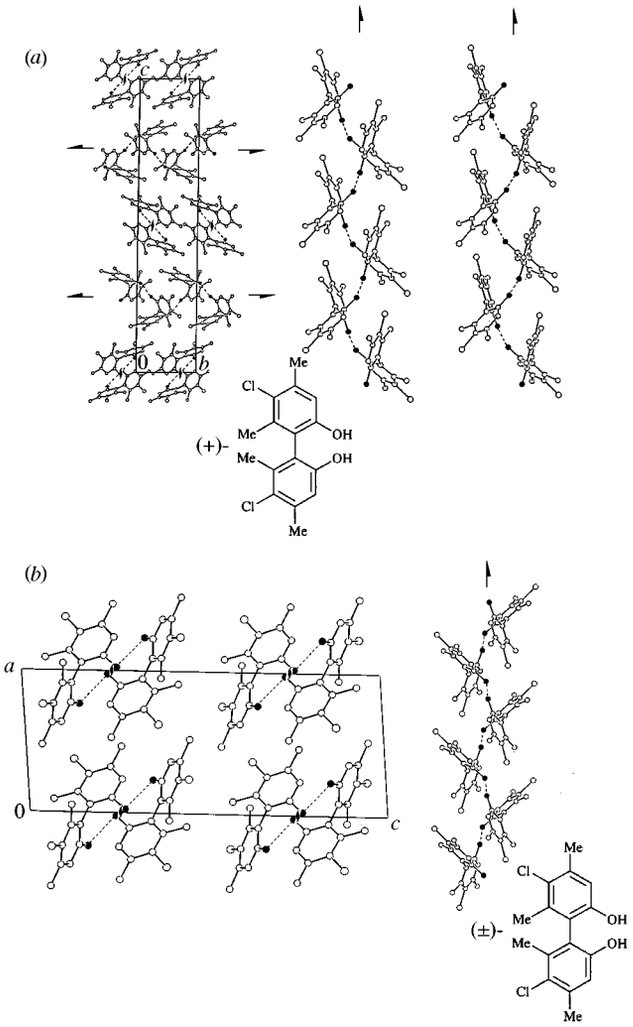

Fig. 4 (*a*) View of the crystal structrure of **7b** along the *a*-axis and side view of the two independent helical structures formed by hydrogen bonding along the *a*- and *b*-axes. (*b*) View of the crystal structure of **7c** along the *b*-axis and side view of the 2_1 helical structure in **7c** crystals. Hydrogen bonds are shown by dotted lines and oxygen atoms by filled circles.

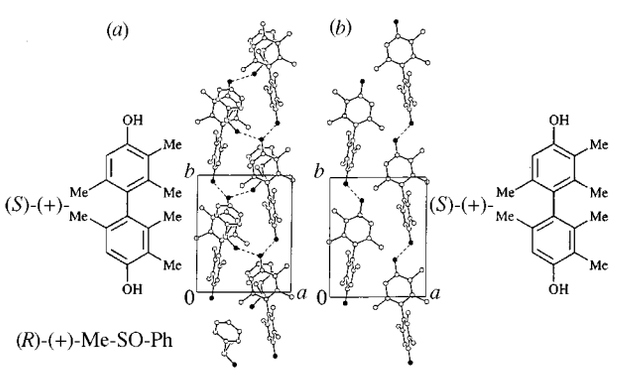

Fig. 5 (*a*) View of the crystal structure of the 1:1 inclusion complex of (*S*)-**8b** and (*R*)-**10b**. (*b*) View of the same structure as that shown in (*a*), but guest molecules, **10b**, excluded for clarity. Hydrogen bonds are shown by dotted lines and oxygen atoms by filled circles.

molecules along the *b*-axis. The same type of linear arrangement of **8b** probably would be formed in chiral and racemic crystals of **8**, although no direct structure analysis is available for either **8b** or **8c** crystals.[19]

Formation of 11c, 12c and 14c in the solid state

When IR spectra of a 1:1 mixture of **11a** and **11b** were measured every 30 min for 3 h, the original OH absorption at 3275 cm^{-1} turned into that of **11c** at 3410 cm^{-1}. Interestingly, mixing of **11b** and **12a** in a 1:1 ratio in the solid state gave a mixed racemic compound of **11b** and **12a**. By measurement of IR spectra of a 1:1 mixture of **11b** (3275 cm^{-1}) and **12a** (3275 cm^{-1}) every 15 min for 1.5 h, the original OH absorptions changed into those of the mixed racemic compound at 3400 cm^{-1}. The IR spectrum of the 1:1 mixed racemic compound (mp 191 °C) of **11b** (mp 127 °C) and **12a** (mp 138 °C) was identical to that prepared by crystallization of **11b** and **12a** from toluene and the mp of the racemic compound was rather higher than that of each component as indicated. By similar IR spectral measurement of a 1:1 mixture of **11b** and **14a** every 15 min for 2 h, OH absorptions of **11b** (3275 cm^{-1}) and **14a** (3255 cm^{-1}) turned into those of their mixed racemic compound (3410 cm^{-1}). The mp of the racemic compound (mp 193 °C) was also much higher than that of **11a** (mp 127 °C) or **14a** (mp 100 °C). However, the acetylenic diol **16c**, which has *tert*-butyl substituents instead of the aryl groups present in **11**, **12** and **14**, did not show any tendency towards molecular movement in the solid state. This is not due to the bulk of the *tert*-butyl group, because **15** which has hydrogen substituents also did not show any such behavior. In order to study the mechanism of this molecular movement in the solid state, X-ray structural study of these crystals was carried out.

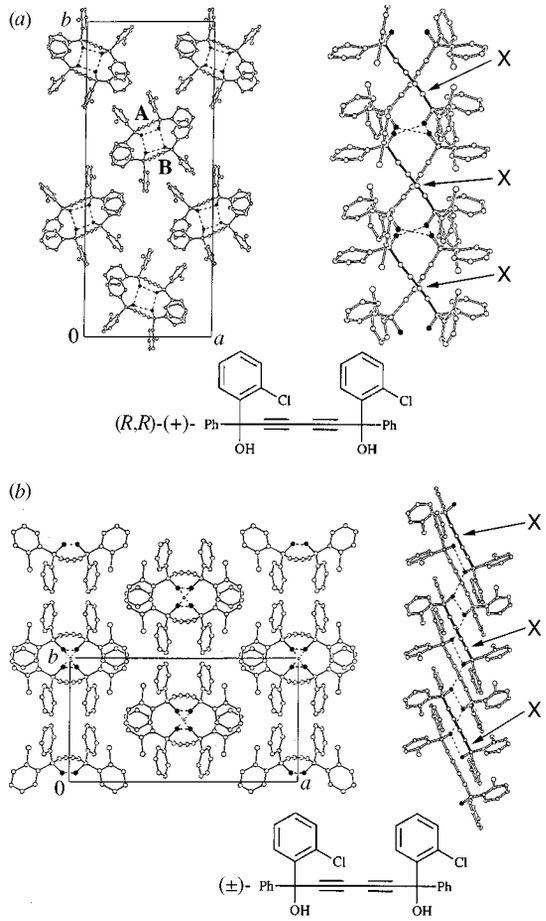

Fig. 6 (*a*) View of the crystal structure of **11b** along the *c*-axis and side view of the molecular column characterized by the cyclic hydrogen bonds among four hydroxy groups of four neighboring molecules. (*b*) View of the crystal structure of **11c** along the *b*-axis and side view of the molecular column consisting of **11a** and **11b** molecules in **11c** crystals. Hydrogen bonds are shown by dotted lines and oxygen atoms by filled circles.

In **11b** crystals, two independent molecules **A** and **B** (see Fig. 6) stack along the *c*-axis to form a molecular column with a hydrophilic interior and hydrophobic exterior. The center of the column is penetrated by a non-crystallographic two-fold axis. In racemic crystals of **11c**, the molecules related by centers of

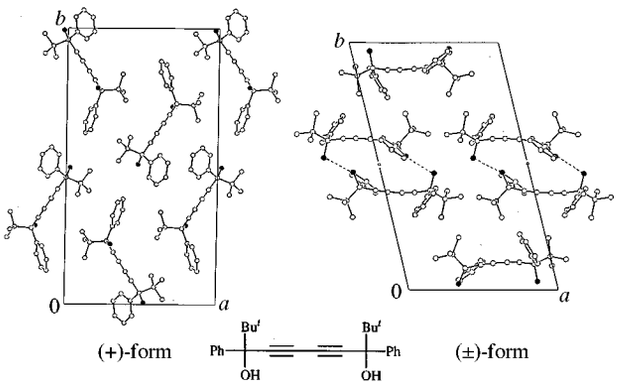

Fig. 7 (*a*) View of the crystal structure of **16b** along the *c*-axis. (*b*) View of the crystal structure of **16c** along the *b*-axis. Hydrogen bonds are shown by dotted lines and oxygen atoms by filled circles.

symmetry stack along the *c*-axis to make a molecular column with a hydrophilic interior and hydrophobic exterior. All the hydroxy groups located in the inside of the columns participate in hydrogen bonds as donors and acceptors, generating hydrophilic cores in the center of the columns.

The side view of the molecular columns in **11b** and **11c** crystals is shown in Fig. 6. These two molecular columns look quite different from each other but have similar structural components. The columns in **11b** crystals are separated into two identical zigzag chains by breaking the hydrogen bonds between molecules **A** and **B**. One of these chains is labelled X in Fig. 6 and the other is unlabelled. These zigzag chains are formed by the repetition of head-to-tail hydrogen bonds. Similarly, the columns in **11c** crystals consist of two zigzag chains with opposite chirality, by breaking the hydrogen bond between **11a** and **11b** molecules. The zigzag chain (labelled X) of **11b** in the **11c** crystals is similar to that (labelled X) in the **11b** crystals. The molecular column in **11b** crystals is modelled by combining two zigzag chains of the same chirality so that a cyclic hydrogen bond may be formed. The molecular column in **11c** crystals is modelled by combining (+)- and (−)-zigzag chains so that a continuous hydrogen bond chain, ···O–H···O–H··· O–H···, may be formed.

The construction of the hydrophobic columns in **11c** crystals can be imagined by mixing the columns in **11a** and **11b**, separating each column into two zigzag chains, pairing the (+) and (−) chains to make new columns and rearranging them. The structure solution of **11b** is poor because of severe crystal decay during data collection and therefore detailed comparison of hydrogen bonds between **11b** and **11c** is meaningless. However, the density of **11b** crystals is much smaller than that of **11c** crystals, implying that the intercolumn packing in **11c** will be more favorable than that in **11b**.

The structure of the mixed racemic crystals of **11b** and **12a** was determined by X-ray analysis. The structure was isomorphous with that of **11c**. The replacement of **11a** molecules in **11c** crystals by **12a** molecules gives the mixed racemic crystals consisting of **11b** and **12a** molecules. The **12a** crystals will be isomorphous with those of **11a**. The transformation of a powdered mixture of **11b** and **12a** into the mixed racemic crystals will be essentially the same as that in **11**.

The crystal structures of **16b** and **16c** are shown in Fig. 7. The powdered enantiomer crystals of **16a** and **16b** are not transformed into the racemic crystals. The racemic crystals of **16c** were formed by recrystallization of **16a** and **16b** from toluene. Interestingly, no intermolecular hydrogen bond is observed in **16b** crystals, while cyclic dimers are formed around the centers of symmetry by hydrogen bonding in **16c** crystals. There is no common packing mode between **16b** and **16c**. Since the density of **16b** is quite large compared with that of **16c** and the diacetylenic rod of **16a** or **16b** in the racemic crystal is not straight but curved due to steric strain, possibly, because of the formation

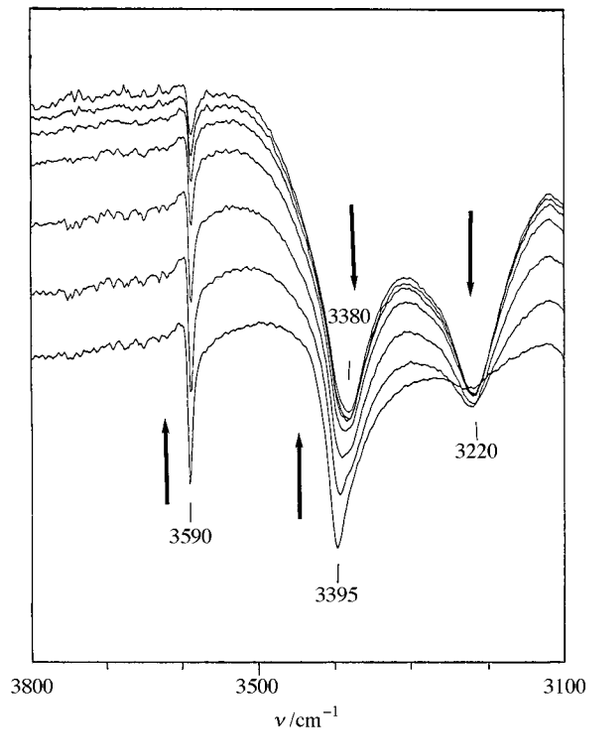

Fig. 8 IR spectra of a 1:1 mixture of **18a** and **18b**. Measured every 10 min for 1 h in a Nujol mull

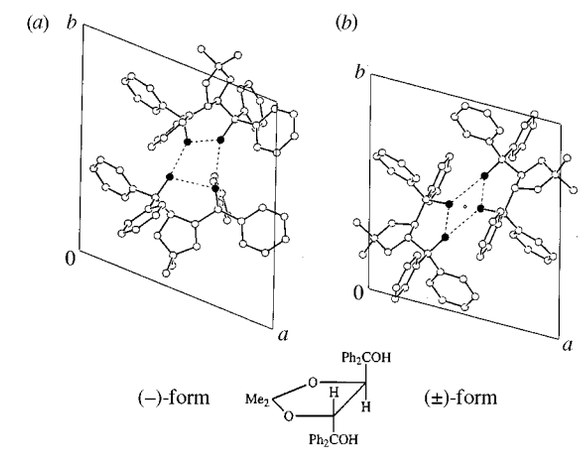

Fig. 9 (*a*) View of the hydrogen bonded dimer formed by two independent molecules in **17a** crystals. (*b*) View of the centric hydrogen bonded dimer formed by **17a** and **17b** molecules in **17c** crystals. Hydrogen bonds are shown by dotted lines and oxygen atoms by filled circles.

of a cyclic dimer by hydrogen bonding, the molecular packing in the chiral crystals of **16b** would be more favorable than that in the racemic crystals of **16c**. It is possible that the packing of the chiral crystal is so good that the formation of the cyclic hydrogen-bonded dimer might not induce transformation from the mixture of enantiomeric crystals to racemic crystals.

Formation of 17c, 18c and 19c in the solid state

When IR spectra of a 1:1 mixture of **18a** and **18b** were measured in a Nujol mull every 10 min for 1 h, the original OH absorptions at 3395 and 3590 cm^{-1} disappeared and new absorptions of **18c** at 3380 and 3220 cm^{-1} appeared (Fig. 8). By similar measurement of a 1:1 mixture of **17a** and **17b** for 2 h, the original absorptions at 3445 and 3210 cm^{-1} turned into those of **17c** at 3425 and 3230 cm^{-1}. By similar measurement of a 1:1 mixture of **19a** and **19b** for 2.5 h, the original OH absorptions at 3530 and 3340 cm^{-1} turned into those of **19c** at 3370 and 3215 cm^{-1}.

The crystal structures of **17a** and **17c**, **18a** and **18c**, and **19a** and **19c** are displayed in Figs. 9, 10 and 11, respectively. The

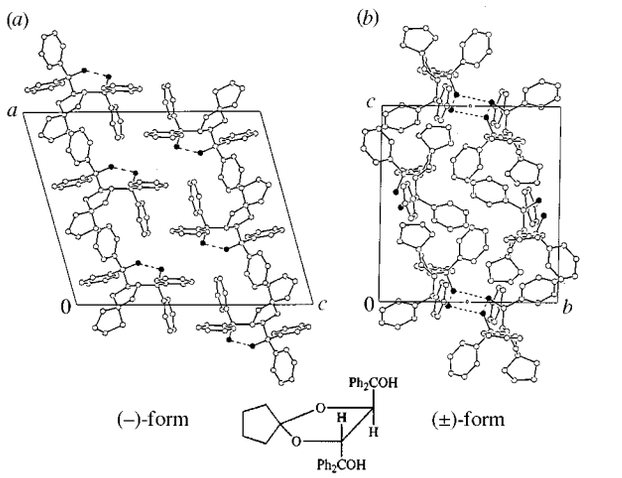

Fig. 10 (*a*) View of the crystal structure of **18a** along the *c*-axis. (*b*) View of the centric hydrogen bonded dimer formed by **18a** and **18b** molecules in **18c** crystals. Hydrogen bonds are shown by dotted lines and oxygen atoms by filled circles.

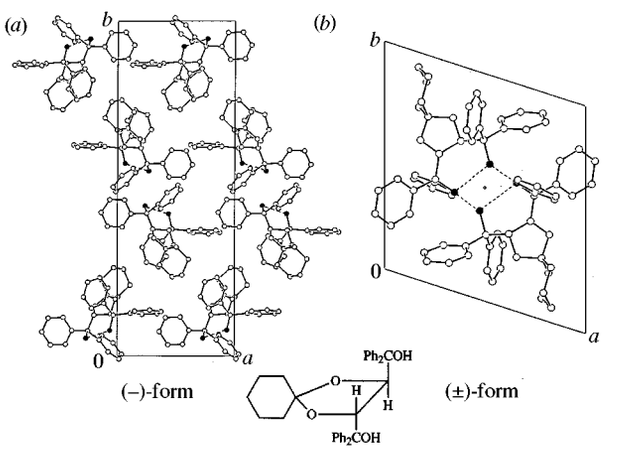

Fig. 11 (*a*) View of the crystal structure of **19a** along the *c*-axis. (*b*) View of the centric hydrogen bonded dimer formed by **19a** and **19b** molecules in **19c** crystals. Hydrogen bonds are shown by dotted lines and oxygen atoms by filled circles.

molecules in these crystals have intramolecular hydrogen bonds between two hydroxy groups. In all racemic crystals, **17c**, **18c** and **19c**, the two molecules related by a center of symmetry form a hydrogen bonded dimer. The hydrophilic groups are concentrated in the interior of the dimer to make a closed hydrogen bonded loop while the exterior of the dimer is hydrophobic and no inter-dimer hydrogen bond is formed.

In **17a** crystals, there are two independent molecules per unit cell (Fig. 9). These two molecules related by a pseudo two-fold axis are hydrogen bonded to give a dimeric structure with a hydrophilic interior and a hydrophobic interior. There is no hydrogen bond between the dimers. The distances of intra- and inter-molecular hydrogen bonds are 2.611 and 2.620 Å, and 2.740 and 2.735 Å, respectively. The angles (O–H · · · O) of the intramolecular hydrogen bonds are 173 and 170°, while the angles of intermolecular hydrogen bonds are 137 and 133° (which deviate considerably from 180°). In **17c** crystals, the distances and angles of intra- and inter-molecular hydrogen bonds are 2.616 and 2.722 Å, and 165 and 147°, respectively. The intermolecular hydrogen bond in **17c** crystals is shorter in length and geometrically more favorable than that in **17a**, and the density of **17c** is significantly larger than that of **17a**.

In **18a** crystals, no intermolecular hydrogen bond is observed (Fig. 10). The distance and angle of the intramolecular hydrogen bond are 2.706 Å and 155°, respectively. A subtle competition between van der Waals interactions and hydrogen bonding interactions determines whether the hydrogen bonded dimer is formed or not. The formation of the closed hydrogen bonded loop is geometrically strained as observed in **17a** crystals and the molecule is mostly hydrophobic, suggesting that the sum of the dispersion forces is fairly large. In **18c** crystals, the distances and angles of intra- and inter-molecular hydrogen bonds are 2.639 and 2.723 Å, and 174 and 149°, respectively. The conversion of the mixed crystals of **18a** and **18b** into **18c** crystals is at least in part due to the formation of the hydrogen bonded dimer in **18c** crystals, although the density of **18c** is slightly smaller than that of **18a**.

Also in **19a** crystals, no intermolecular hydrogen bond is observed (Fig. 11). The distance and angle of the intramolecular hydrogen bond are 2.681 Å and 169°, respectively. In **19c** crystals, the distances and angles of intra- and intermolecular hydrogen bonds are 2.612 and 2.733 Å, and 163 and 159°, respectively. Since the hydrogen bonded dimers are formed in **19c** and the density of **19c** crystals is significantly larger than that of **19a** crystals, the molecular assembly in **19c** will be more favorable than that in **19a** crystal.

It is clear that the molecular movement in the solid state is accelerated in Nujol mulls, since the formation of **18c** from **18a** and **18b** in the absence of Nujol takes 20 days. The molecular movement of **17**–**19** in the solid state occurs much faster in the presence of liquid alkanes such as hexane, tetradecane, hexadecane, octadecane; a haloalkene such as hexachlorobutadiene; seed oils such as olive, rapeseed, coconut, and soybean oil; and artificial oils such as silicone oil. In the presence of the liquid, crystals of the racemic compound were formed immediately after mixing the chiral crystals. Water also accelerated the molecular movement; for example, **17c** was formed from **17a** and **17b** in the presence of water within 8 days.

Formation of 20c, 21c, 22c, 23c and 24c in the solid state

The easy molecular movement between two enantiomer crystals in the presence of a liquid is not limited to particular diol host compounds. In fact, the phenomenon can be observed for a rather wide variety of chiral compounds. By successive IR spectral measurement of a 1:1 mixture of **20a** and **20b** in Nujol mulls for 7 days, the original OH absorptions at 3405 and 3335 cm^{-1} turned into those of **20c** at 3410 and 3360 cm^{-1}. However, molecular movement of the dimethyl ester of **20** (**21**) occurred much faster. Within 3 h, the OH absorptions of **21a** and **21b** at 3475, 3415 and 3370 cm^{-1} turned into those of **21c** at 3530 and 3460 cm^{-1}. Monohydroxycarboxylic acids **22** and **23** also showed similar behaviour in the solid state. Within 24 h, OH absorptions of a 1:1 mixture of **22a** and **22b** at 3530 and 3385 cm^{-1} turned into those of **22c** at 3440 cm^{-1}. Similarly, within 2 h, the OH absorption of a 1:1 mixture of **23a** and **23b** turned into that of **23c** at 3395 cm^{-1}. The molecular movement occurs more rapidly in a 1:1 mixture of norephedrine enantiomers **24a** and **24b**, and their OH absorptions at 3335 and 3270 cm^{-1} turned into those of **24c** at 3330 and 3270 cm^{-1} within 3 min.

Conclusion

By mixing powdered (−)- and (+)-enantiomer crystals in the solid state, new crystals of the racemic compound were formed quite easily by molecular movement between the two enantiomer crystals. When the mixing was carried out in the presence of liquids such as liquid paraffin, seed oils, silicone oil or water, the molecular movement occurred very fast and sometimes the formation of the racemic crystal was completed within a few minutes. It will be an extremely interesting and important research topic to investigate how these liquids carry such molecules in the solid state. X-Ray structural study of crystals of both the enantiomeric and racemic compound showed that a complex blending and accurate arrangement of molecules are necessary in order to form a new racemic compound crystal. Helical structures or molecular columns with a hydrophobic

exterior are observed in the chiral crystals of **1**, **5**, **7** and **11**. When powdered (−)- and (+)-enantiomer crystals are mixed, these hydrophobic structural units might diffuse to each other through the interface between the enantiomer crystals and be rearranged to make the corresponding racemic crystals. The energy required to separate the molecular column into the zig-zag chains will be compensated by the formation of new hydrogen bonds between the (−)- and (+)-chains. Because there is no intermolecular hydrogen bond in the chiral crystals of **18** and **19**, the racemic crystals might be created just by the diffusion of the enantiomer molecules through the interface, followed by the formation of the centrosymmetric dimers. The dimers in the chiral crystals of **17** might easily migrate through the interface, because only van der Waals interactions exist between the dimers. Thus, it is speculated that whenever the free energy of a chiral crystal is larger than that of the racemic crystal and the energy barrier of molecular movement through the interface is low, the powdered enantiomer crystals are transformed into the racemic crystals. It is surprising that such accurate blending and arrangement of molecules occur so fast in the solid state.

Acknowledgements

The authors would like to thank the Ministry of Education, Science and Culture, Japan, for a Grant-in-Aid for Scientific Research on Priority Areas, No. 06242105 and 06242107.

Supporting information available: complete tables of the atomic coordinates, thermal parameters, bond angles, and bond distances for **1a**, **1c**, **5b**, **5c**, **7b**, **7c**, **8b**, **10b**, **11b**, **11c**, **12a**, **16b**, **16c**, **17a**, **17c**, **18a**, **18c**, **19a** and **19c** have been deposited with the Cambridge Crystallographic Data Centre (CCDC). For details of the deposition scheme, see 'Instructions for Authors', *J. Chem. Soc., Perkin Trans. 2*, 1997, Issue 1. Any request to the CCDC for this material should quote the full literature citation and the reference number 188/83.

References

1 F. Toda, *Synlett*., 1993, **5**, 303; *Acc. Chem. Res*., 1995, **28**, 480.
2 G. Kaupp, M. Haak and F. Toda, *J. Phys. Org. Chem*., 1995, **8**, 545.
3 F. Toda, K. Tanaka and A. Sekikawa, *J. Chem. Soc., Chem. Commun*., 1987, 279.
4 F. Toda, *J. Synth. Org. Chem. Jpn*., 1990, **48**, 494.
5 F. Toda, K. Tanaka, T. Okada, S. A. Bourne and A. R. Nassimbeni, *Supramol Chem*., 1994, **3**, 291; F. Toda, *Bioorg. Chem*., 1991, **19**, 157.
6 F. Toda, K. Mori, Y. Matsuura and H. Akai, *J. Chem. Soc., Chem. Commun*., 1990, 1591.
7 F. Toda and Y. Tohi, *J. Chem. Soc., Chem. Commun*., 1993, 1238.
8 F. Toda and H. Takumi, *Enantiomer*, 1996, **1**, 29.
9 F. Toda, H. Miyamoto and K. Kanemoto, *J. Chem. Soc., Chem. Commun*., 1995, 1719; F. Toda, *Pure Appl. Chem*., 1996, **68**, 285.
10 A. O. Patil, D. Y. Curtin and I. C. Paul, *J. Am. Chem. Soc*., 1984, **106**, 348; J. R. Scheffer, Y.-F. Wong, A. O. Patil, D. Y. Curtin and I. C. Paul, *J. Am. Chem. Soc*., 1985, **107**, 4898.
11 H. Sato and T. Yasuniwa, *Bull. Chem. Soc. Jpn*., 1973, **47**, 368; J. P. Farges, A. Brau and P. Dupuis, *Solid State Commun*., 1985, **54**, 531; J. P. Singh, R. J. Singh and N. P. Singh, *Tetrahedron*, 1994, **50**, 6441.
12 J. P. Farges and A. Brau, *Physica*, 1986, **143B**, 324; A. Brau, J. P. Farges and A. Sahraoui, *Mol. Cryst. Liq. Cryst*., 1988, **156**, 223; F. A. Sahraoui, J. P. Farges and A. Brau, *Appl. Phys. Commun*., 1989, **65**, 9; M. Salle, M. Jubault, A. Gorgues, K. Boubekeur, M. Fourmigue, P. Bastail and E. Canadell, *Chem. Mater*., 1993, **5**, 1196; A. Brau, J. P. Farges, E. Ghezzal and A. Mammou, *Mol. Cryst. Liq. Cryst*., 1993, **273**, 436; F. Toda and H. Miyamoto, *Chem. Lett*., 1995, 861. In the last paper, it was reported that this phenomenon was found by Toda and Miyamoto, but recently we realised that the phenomenon was discovered by several research groups cited in the literature. We apologize to these authors, especially Professor A. Gorgues, for lack of citation of their work.
13 V. R. Pedireddi, W. Jones, A. P. Chorlton and R. Docherty, *J. Chem. Soc., Chem. Commun*., 1996, 987.
14 F. Toda, K. Tanaka and S. Iwata, *J. Org. Chem*., 1989, **54**, 3007.
15 K. Tanaka, T. Okada and F. Toda, *Angew. Chem., Int. Ed. Engl*., 1993, **32**, 1147.
16 J. Jaques, C. Fouquay and R. Viterbo, *Tetrahedron Lett*., 1971, 4617.
17 W. H. Pirkle and J. L. Schreiner, *J. Org. Chem*., 1981, **46**, 4988.
18 F. Toda and K. Tanaka, *Tetrahedron Lett*., 1988, **29**, 551.
19 K. Tanaka, A. Moriyama and F. Toda, *J. Chem. Soc., Perkin Trans. 1*, 1996, 603.
20 T. Higashizima, N. Sakai, K. Nozaki and H. Takaya, *Tetrahedron Lett*., 1994, **35**, 2023.
21 Chiralpak AS is available from Daicel Chemical Industries Co. Ltd., Himeji, Japan.
22 F. Toda, K. Tanaka, T. Omata, K. Nakamura and T. Oshima, *J. Am. Chem. Soc*., 1983, **105**, 5151.
23 F. Toda, K. Tanaka, H. Ueda and T. Oshima, *Israel J. Chem*., 1985, **25**, 1338.
24 F. Toda, S. Matsuda and K. Tanaka, *Tetrahedron Asymmetry*, 1991, **2**, 983.
25 D. Seebach, A. K. Beck, R. Imwinkelreid, S. Roggo and A. Wonnacott, *Helv. Chim. Acta*, 1987, **70**, 954.
26 G. M. Sheldrick, in *Crystallographic Computing 3*, ed. G. M. Sheldrick, C. Kruger and R. Goddard, Oxford University Press, 1985, pp. 175–189; M. C. Burla, M. Camalli, G. Cascarano, C. Giacovazzo, G. Polidori, R. Spagna and D. Viterbo, *J. Appl. Crystallogr*., 1989, **22**, 389.
27 teXsan: Crystal Structure Analysis Package, Molecular Structure Corporation, 1985 and 1992.
28 K. Mori, Y. Masuda and S. Kashino, *Acta Crystallogr., Sect. C*, 1993, **49**, 1224.
29 I. Goldberg, Z. Stein, E. Weber, N. Dorpinghaus and S. Franken, *J. Chem. Soc., Perkin Trans. 2*, 1990, 953.

Paper 6/06561I
Received 24*th September* 1996
Accepted 26*th March* 1997